AIAA JOURNAL
Vol. 50, No. 8, August 2012

Formation and Structure of Steady Oblique and Conical Detonation Waves

Jimmy Verreault* and Andrew J. Higgins†
McGill University, Montreal, Quebec H3A 2K6, Canada
and
Robert A. Stowe‡
Defence Research and Development Canada–Valcartier, Quebec, Quebec, G3J 1X5, Canada

DOI: 10.2514/1.J051632

The formation and structure of oblique detonation waves initiated by semi-infinite wedges and cones are presented. For wedge or cone angles less than the deflection angle required for an oblique Chapman–Jouguet (CJ) detonation, different wave structures have been previously reported. Using the method of characteristics and numerical simulations, it is shown that, for such low wedge or cone angles, a CJ oblique detonation is eventually initiated following an induction process. It its thus demonstrated that shock-induced combustion with the reaction front remaining uncoupled to the oblique shock in the far field is not a valid solution. Simulations with semi-infinite cones reveal that the effect of the front curvature around the cone axis allows oblique detonations to be formed at angles lower than that of a planar CJ oblique detonation.

Nomenclature

a	=	sound speed
E	=	specific energy
E_a	=	activation energy
k	=	preexponential factor
M	=	Mach number
p	=	pressure
Q	=	dimensionless heat release
T	=	temperature
U	=	velocity magnitude
u	=	x-velocity component
v	=	y-velocity component
X	=	abscissa coordinate
Y	=	ordinate coordinate
β	=	oblique shock or detonation wave angle
γ	=	ratio of specific heats
θ	=	deflection angle
λ	=	reaction progress variable
ρ	=	density
ϕ	=	flow angle
ω	=	reaction rate

I. Introduction

THE oblique detonation wave engine concept offers the potential for greater efficiency at higher Mach numbers [1,2] in comparison with the traditional scramjet. This potential is achieved by using a standing oblique detonation wave (ODW) as the combustor, thereby reducing the length of the engine and minimizing drag losses. A series of extensive numerical studies were conducted in the last decade at the University of Toronto Institute for Aerospace Studies [3–6]. Their research aimed at optimizing the supersonic mixing between the injected gaseous fuel with the airstream, preventing premature ignition of the mixture in the engine inlet and ensuring that the overall propulsion device provided positive thrust for realistic flight conditions. In this concept, the key challenge is the ability to initiate an ODW at the desired location and to stabilize it over the entire flight time. If prompt combustion in a supersonic stream can be effected via shock-induced combustion without the large total pressure losses associated with ODWs, potentially even greater efficiencies could be realized. Oblique detonations may also find application in the superdetonative mode of ram accelerators, a hypervelocity launcher concept in which a projectile that resembles the center body of an axisymmetric scramjet accelerates as it flies down a tube filled with a premixed combustible gas [7,8]. Reviews on oblique detonation waves and their application to hypersonic propulsion were reported by Shepherd [9] and Powers [10].

An essential first step in examining the ODW is to determine the possible steady wave structures that may occur. The simplest approach to solve the flow conditions upstream and downstream of an ODW is to treat it as a single discontinuity. The oblique shock and the reaction zone are together assumed to be infinitely thin. The Rankine–Hugoniot equations can then be solved across the ODW. This type of analysis was first reported in the 1950s [11,12] and was concisely summarized by Gross [13]. Gross constructed detonation polars by relating the downstream flow conditions to the deflection angle. The polars thus represent the solution of the Rankine–Hugoniot relations showing the possible wave angles corresponding to a given deflection angle. Pratt et al. [14] also reported such an analysis, and their terminology is adopted here. A typical example of shock and detonation polars is shown in Fig. 1. There is a minimum ODW angle $\beta = \beta_{CJ}$ for which a solution to the reactive Rankine–Hugoniot relations exists. At this value β_{CJ}, a unique solution is obtained: the Chapman–Jouguet (CJ) solution. For this case, the upstream velocity normal to the shock is equal to the CJ velocity of the mixture, the downstream Mach number normal to the shock is unity, and the deflection angle is θ_{CJ}. For $\beta > \beta_{CJ}$, the upstream velocity normal to the shock is greater than the CJ value, and two solutions are obtained for the downstream conditions. The solution corresponding to a smaller deflection angle is characterized by a supersonic downstream velocity normal to the shock. This class of ODW is referred to as weak underdriven. A wave structure schematic corresponding to a weak underdriven oblique detonation is shown in Fig. 2a. The other solution corresponding to a larger deflection angle has a subsonic downstream velocity normal to the shock. This class is

Presented as Paper 2011-5546 at the 47th AIAA/ASME/SAE/ASEE Joint Propulsion Conference & Exhibit, San Diego, CA, 31 July–3 August 2011; received 21 September 2011; revision received 26 January 2012; accepted for publication 9 February 2012.

*Graduate Student, Department of Mechanical Engineering. Student Member AIAA.
†Associate Professor, Department of Mechanical Engineering. Senior Member AIAA.
‡Propulsion Group Leader. Senior Member AIAA.

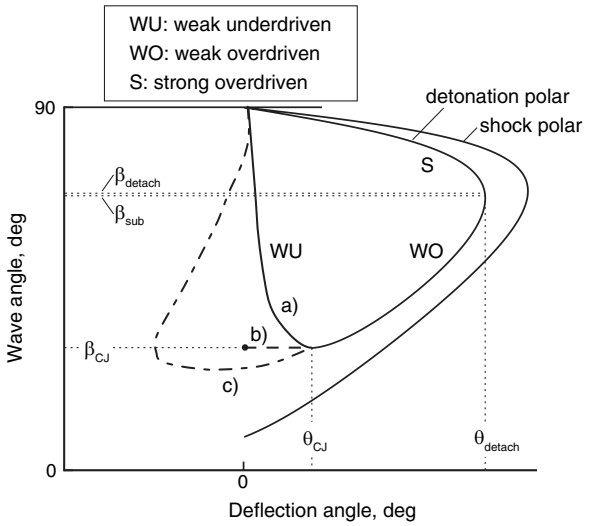

Fig. 1 Typical shock and detonation polars. Lines a), b), and c) refer to different wave structures for deflection angles less than θ_{CJ}, which are illustrated in Fig. 2.

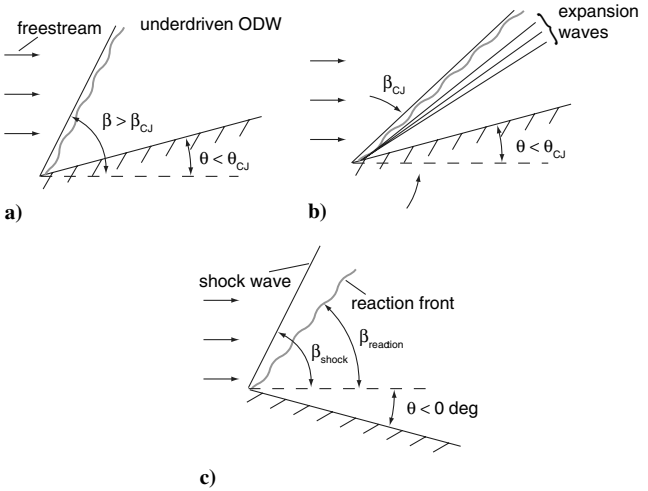

Fig. 2 Schematic of different wave structures for deflection angles less than θ_{CJ}: a) underdriven oblique detonation, b) CJ oblique detonation followed by expansion waves, and c) two-wave shock/reaction structure.

subdivided into two types of ODW depending on whether β is lesser or greater than β_{detach} (the ODW angle corresponding to θ_{detach}, the maximum deflection angle for which an ODW can remain attached). For $\beta < \beta_{detach}$, the deflection angle is in the range $\theta_{CJ} < \theta < \theta_{detach}$, and this class is known as weak overdriven. In this range of deflection angle, although the normal velocity downstream of the reaction zone is subsonic, the velocity magnitude is supersonic. The downstream velocity magnitude becomes subsonic for ODW angles larger than β_{sub}, which is slightly lower than β_{detach} (generally less than 1 deg lower). For $\beta > \beta_{detach}$, the ODW is referred to as strong overdriven.

Based on this analysis, Pratt et al. [14] concluded that, for an ODW to be stabilized, the deflection angle must be in the range $\theta_{CJ} < \theta < \theta_{detach}$, and a CJ or weak overdriven ODW would result. For $\theta < \theta_{CJ}$, they concluded that weak underdriven ODWs cannot be realized because the Mach waves originating from the wedge surface are at a lower angle than the oblique shock, and thus, the presence of the wedge is not transmitted to the shock. Also, other researchers, such as Buckmaster and Lee [15], Ashford and Emanuel [16], and Emanuel and Tuckness [17], ruled out the weak underdriven solution branch based on the fact that a flow being accelerated from subsonic to supersonic velocities only by heat addition violates the second law of thermodynamics. However, Powers and Gonthier [18] showed that weak underdriven detonations can in fact be obtained if the reaction scheme involves an exothermic reaction followed by an endothermic one. In such a case, the heat release and the sonic parameter $(1 - M^2)$ are simultaneously zero at a critical saddle point, and the endothermic reactions proceed to completion downstream of this point. This phenomenon has been widely discussed for the case of planar detonations with exothermic/endothermic reactions known as pathological detonations (see Fickett and Davis [19] and Lee [20]).

To provide a physical solution likely to be observed in experiments, Ashford and Emanuel [16] and Emanuel and Tuckness [17] suggested that, for deflection angles $\theta < \theta_{CJ}$, an ODW is formed at the CJ angle β_{CJ}, and rarefaction waves follow the reaction zone to expand the flow and bring it parallel to the wall-deflection angle θ. This behavior is illustrated in Fig. 1 with the dashed line b, and the corresponding wave structure is shown in Fig. 2b. Buckmaster and Lee [15] also solved the reactive Rankine–Hugoniot equations to construct polars. They considered a wave structure consisting of a reaction front that could be at a lower angle than that of the inert oblique shock. This structure intended to mimic the situation where a flame (or a deflagration) is located between a wedge and an oblique shock, which was observed, for example, in the two-layer detonation experiment [21]. Under these assumptions, the Rankine–Hugoniot equations were solved twice, once across each front. The polars they obtained showed that the two-front structure could be formed even for negative deflection angles, which is shown in Fig. 1 with the dash-dot line c and in Fig. 2c. The wave structure considered by Buckmaster and Lee [15] is different than the case of shock-induced combustion in that chemical reactions are triggered by some phenomena other than the oblique shock. If shock-induced combustion were considered, that is if the mixture is self-ignited by the temperature jump across the oblique shock, the induction length behind a straight shock would be the same for all streamlines, and the reaction front would be parallel to the shock. It is thus important to point out that, for shock-induced combustion, the reaction front cannot be at a lower angle than that of the shock.

The formation process of an ODW attached to a wedge was first addressed by Li et al. [22]. They performed numerical simulations with detailed chemistry to show the global flow features of the ODW-formation process, which are presented in Fig. 3. Li et al. [22] showed the presence of a thermally neutral induction zone behind the oblique shock at the tip of the wedge. Near the end of the induction zone, exothermic reactions were triggered, sending compression waves towards the oblique shock that strengthened it. The induction length behind the oblique shock was thus sharply reduced, which marked the onset of an ODW.

Ghorbanian and Sterling [23] reported a theoretical analysis on the possible wave structures induced by a double-ramp configuration, where the angle of the first and second ramps (θ_w and θ_b) were independently varied. The length of the first ramp corresponded exactly to the length of the induction zone. According to their model,

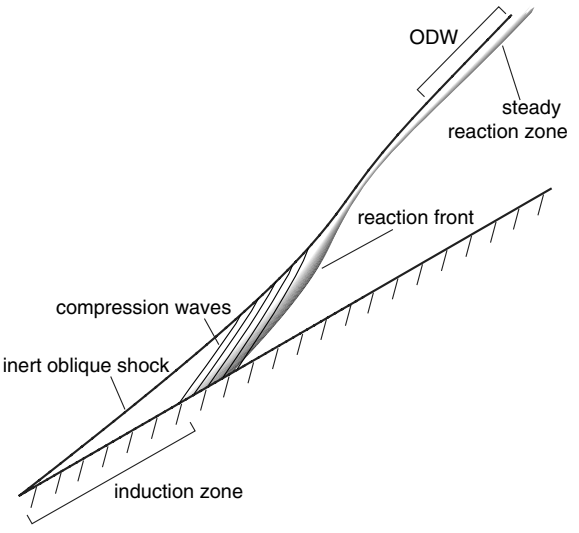

Fig. 3 Schematic of the formation process of an ODW.

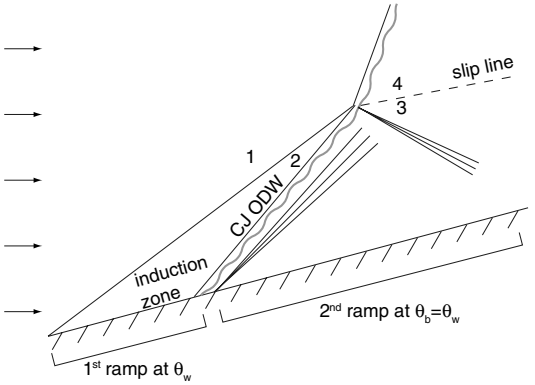

Fig. 4 Wave structure for the formation of an ODW, as suggested by Ghorbanian and Sterling [21].

for the case of a semi-infinite wedge (which is a special case with $\theta_w = \theta_b$), the induction zone was followed by a CJ ODW that originated from the wedge surface and interacted with the oblique shock. The wave structure for this case is illustrated in Fig. 4. The goal of their study was to identify steady ODW solutions admitted by a Rankine–Hugoniot analysis, defined in other studies as $\theta_{CJ} < \theta < \theta_{detach}$. Considering the formation wave structure of an attached ODW, they suggested two additional requirements for the existence of steady ODWs. The first consisted of a Mach number in region 2 (see Fig. 4) greater than the CJ Mach number (calculated with the flow conditions of region 2). The second requirement was obtained by pressure-matching the flow conditions between regions 3 and 4. Considering these two conditions, the criterion for the existence of steady ODWs was expressed as $0 \le \theta_w \le \theta_{w,s}$, where $\theta_{w,s}$ was in the range $\theta_{CJ} < \theta_{w,s} < \theta_{detach}$. Note that, in the range of deflection angles $0 < \theta_w < \theta_{CJ}$, they concluded that a steady ODW would be obtained.

It is clear that the different wave structures (for a stabilized ODW or for the formation of an ODW) reported in previous studies are due to various assumptions made a priori. This is the case especially for deflection angles $\theta < \theta_{CJ}$. Experimental evidence of ODW stabilization at such low deflection angles was shown by Verreault and Higgins [24] in ballistic range experiments. Therefore, the goal of this work is to clarify the structure of steady ODWs, especially in the range $\theta < \theta_{CJ}$, without a priori imposing of a particular solution. This was achieved by simulating hypersonic reactive flows over wedges and cones using the method of characteristics (MoC) and a computational fluid dynamics environment developed by Quirk [25] called Adaptive Mesh Refinement Interactive Teaching Aid (Amrita).

II. Theoretical and Numerical Models

To simulate the flowfields, the governing equations are the reactive Euler equations in two dimensions, which are expressed in conservative form as follows:

$$\frac{\partial \boldsymbol{W}}{\partial t} + \frac{\partial \boldsymbol{F}}{\partial x} + \frac{\partial \boldsymbol{G}}{\partial y} = \boldsymbol{H} + \boldsymbol{S} \qquad \boldsymbol{W} = \begin{pmatrix} \rho \\ \rho u \\ \rho v \\ \rho E \\ \rho \lambda \end{pmatrix},$$

$$\boldsymbol{F} = \begin{pmatrix} \rho u \\ \rho u^2 + p \\ \rho uv \\ (\rho E + p)u \\ \rho \lambda u \end{pmatrix}, \qquad \boldsymbol{G} = \begin{pmatrix} \rho v \\ \rho uv \\ \rho v^2 + p \\ (\rho E + p)v \\ \rho \lambda v \end{pmatrix}, \qquad (1)$$

$$\boldsymbol{H} = -\frac{\delta}{y}\begin{pmatrix} \rho v \\ \rho uv \\ \rho v^2 \\ (\rho E + p)v \\ \rho \lambda v \end{pmatrix}, \qquad \boldsymbol{S} = \begin{pmatrix} 0 \\ 0 \\ 0 \\ 0 \\ \rho \omega \end{pmatrix}$$

$\boldsymbol{W}$ is the conservative solution vector, $\boldsymbol{F}$ and $\boldsymbol{G}$ are the convective fluxes, and $\boldsymbol{H}$ and $\boldsymbol{S}$ are the geometry and reaction source terms, respectively, with $\delta = 0, 1$ for rectangular and axisymmetric configurations, respectively. λ is the product mass fraction and varies from 0 to 1. The equation of state can be expressed as

$$p = (\gamma - 1)\rho\left[E - \frac{u^2 + v^2}{2} + \lambda Q\right]$$

The chemistry was modeled with an irreversible one-step Arrhenius equation of the following form:

$$\omega = (1 - \lambda)k \exp\left(-E_a \frac{\rho}{p}\right)$$

In this work, the chemistry parameters were set as $\gamma = 1.3$, $Q = 10$, and $E_a = 10$. It can be shown from a linear stability analysis [26] that these parameters provide a stable behavior for a planar CJ detonation. Unstable cases occur for higher activation energies, and the wave structure in this case will be considered in a follow-up publication. The value of the preexponential factor k was adjusted to ensure that the half-reaction length of a planar CJ detonation (the distance between the shock front and the location where $\lambda = 0.5$) was unity.

Figure 5 shows a schematic of the simulation parameters presented in this work, where θ is the wedge angle. The flow conditions were normalized with the freestream pressure $\tilde{p}_o$ and density $\tilde{\rho}_o$. The tilde sign $\tilde{()}$ refers to a dimensional quantity. The nondimensional variables were defined as

$$p = \frac{\tilde{p}}{\tilde{p}_o}, \qquad \rho = \frac{\tilde{\rho}}{\tilde{\rho}_o}, \qquad U = \tilde{U}\sqrt{\frac{\tilde{\rho}_o}{\gamma \tilde{p}_o}} = \frac{\tilde{U}}{\tilde{a}_o}, \qquad a = \sqrt{\frac{\gamma p}{\rho}}$$

$$u = U\cos\phi, \qquad v = U\sin\phi, \qquad M = \frac{U}{a}$$

The freestream conditions were set as

$$p_o = 1, \qquad \rho_o = 1, \qquad u_o = M_\infty = 7, \qquad v_o = 0, \qquad \lambda_o = 0 \qquad (2)$$

A. Method of Characteristics

The MoC program developed for the present study follows closely the method described in Zucrow and Hoffman [27], with the chemistry adapted to the one-step Arrhenius model. For all MoC simulations, the reactive steady-state Euler equations were solved in two dimensions (Eq. (1) with the time derivatives equal to zero), hence imposing a steady flowfield solution. The set of differential equations were cast in the characteristic form, and the obtained set of ordinary differential equations were integrated with a predictor-corrector method. Because of the stiffness of the Arrhenius rate expression to be solved along the streamlines, the flow conditions were solved at the intersection of the C^+ characteristics with the streamlines, and the C^- characteristics were extended backward. A typical characteristics network at the tip of a wedge is shown in Fig. 6a. The network was constructed by tracing a C^+ characteristic from the wall to the oblique shock, which represents the left boundary of the domain. At the shock, the flow conditions were

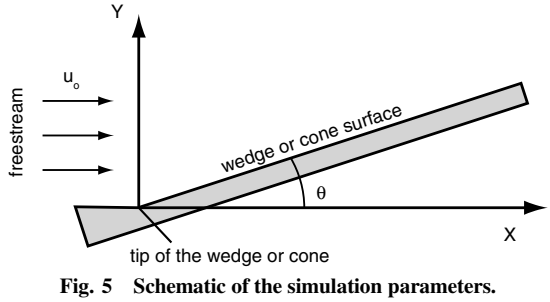

Fig. 5 Schematic of the simulation parameters.

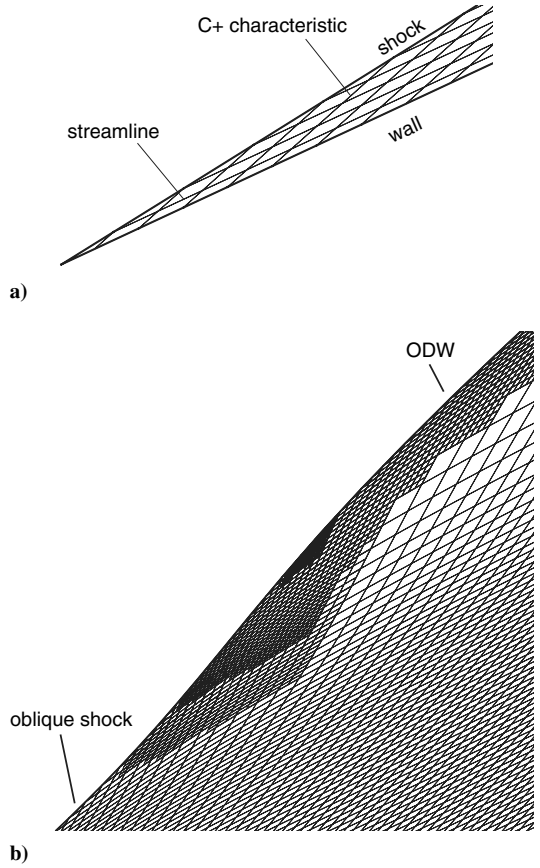

Fig. 6 Typical characteristics networks a) at the tip of a wedge and b) at the onset of an ODW showing the characteristics refinement method.

determined by satisfying the oblique shock relations and the information carried by the C^+ characteristic. This procedure thus corresponds to a shock-tracking method. In the problem of ODW initiation from a wedge, the induction length at the tip of the wedge (along its surface) can be several orders of magnitude larger than the induction length in the ODW reaction zone. It was therefore necessary to increase the number of characteristics where the reaction front coupled with the oblique shock at the onset of the ODW. The MoC program was capable of automatically doubling the number of characteristics with a recursive method based on a specified number of points per half-reaction length (pts/hrl). In the simulations presented in this work, the refinement criteria were set at 2 pts/hrl everywhere in the flowfield and at 10 pts/hrl in the ODW reaction zone. The main advantage of the MoC is that the governing equations are directly integrated along characteristics and streamlines, as opposed to discretized according to a specific scheme for the case of numerical simulations. Therefore, with the MoC program, 10 pts/hrl is sufficient to properly model the reaction zone structure with the parameters of this study. This was verified by doubling the number of characteristics (to 20 pts/hrl), and the difference between this solution and the one with 10 pts/hrl was negligible. An example where the network was refined three times due to the shortening of the induction length as the reaction front coupled to the shock is illustrated in Fig. 6b.

In some cases, characteristics running in the same direction crossed at a location of a large rate of heat release from the chemical reaction. At that location, characteristics merged to form a weak oblique shock, altering part of the characteristic network built before the shock formation. To rebuild the network to account for this shock represented a challenging task. In the simulations presented here, the network constructed before the point where characteristics crossed was not modified; hence, the shock formed was not properly simulated. Despite this limitation, the simulations reached completion, and the effect of using this technique will be investigated by comparing the MoC simulations with the results from Amrita in Sec. III.

B. Amrita Environment

The governing equations for the numerical simulations are given by Eq. (1). The Amrita environment employs a hierarchical system of mesh patches according to a mesh-refinement scheme defined by the user. For the simulations presented in this work, the coarsest mesh, which covered the entire numerical domain, was set such that there was one grid point per half-reaction length. Mesh refinement was automatically applied at the locations of steep gradient to correctly resolve the flowfield. The most refined grid level corresponded to 64 pts/hrl. The Lax–Friedrichs solver was used to evaluate the fluxes in the Euler equations. The complete numerical domain was initialized with the freestream values, and the flow features evolved to their steady state by marching in time. Therefore, both transient and steady phases of a solution were obtained. By comparing the steady phase with a flowfield simulated by the MoC program (which imposed a steady solution), it could be determined whether this flowfield was dynamically stable.

III. Simulation Results

A. Rectangular Configuration

Using the initial conditions given by Eq. (2), a Rankine–Hugoniot analysis was performed to obtain the shock and detonation polars shown in Fig. 7 with the solid lines. No assumption was made for $\theta < \theta_{CJ}$. The symbols represent the results obtained from the MoC program. In a single MoC simulation, the inert oblique shock angle was obtained at the tip of the wedge (where the oblique shock and the reaction front were uncoupled), and the ODW angle was obtained downstream of the coupling point. In the range $\theta_{CJ} < \theta < \theta_{detach}$, the agreement with the Rankine–Hugoniot analysis is excellent. For a deflection angle of $\theta = 15$ deg, the wave angle is 20.9 deg (the value for an inert oblique shock) at the tip of the wedge and becomes 31.5 deg (the value for an oblique detonation) in the far field. The evolution of the wave angle for this case, obtained from the MoC program and Amrita, is illustrated in Fig. 8. For the numerical simulations, the wave angle was calculated by locating the pressure jump across the oblique shock and by considering two grid points that are separated by five grid points along the shock. Also shown in Fig. 8 is the effect of the numerical grid resolution, and it can be observed that 64 pts/hrl in the ODW reaction zone was sufficient to obtain grid-independent results. An excellent agreement between the theoretical and numerical results is observed. The evolution of the

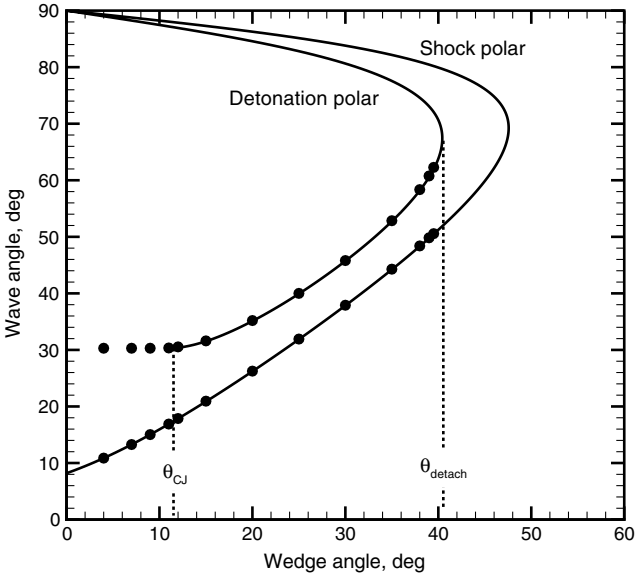

Fig. 7 Shock and detonation polars in the rectangular configuration. Symbols are results from MoC simulations.

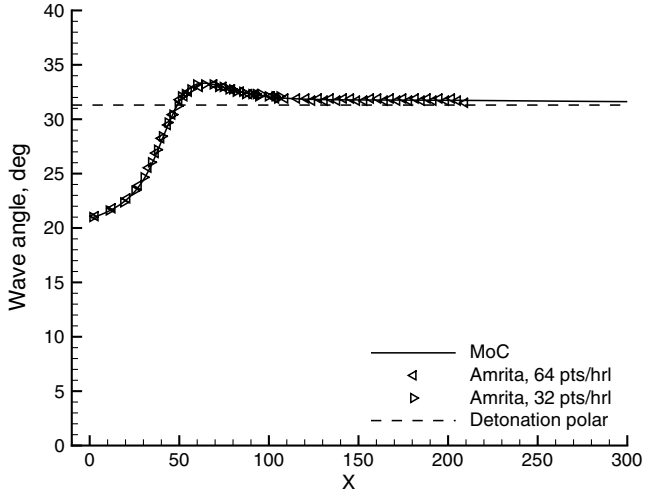

Fig. 8 Evolution of the wave angle $\theta = 15$ deg in the rectangular configuration.

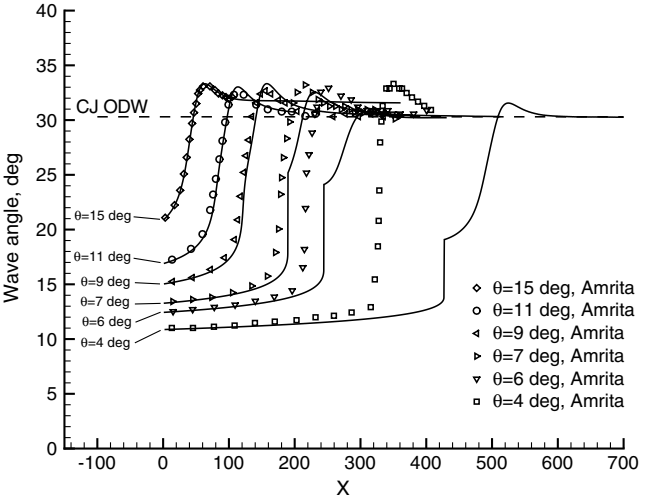

Fig. 9 Evolution of the wave angle 4 deg $< \theta <$ 15 deg in the rectangular configuration. Solid curves and symbols are MoC and Amrita results, respectively.

wave angle shows that downstream of the tip ($X > 0$), compression waves produced by the exothermic reactions interact with the shock and strengthen it. The maximum value of the wave angle is 33.3 deg, where the reaction front couples with the shock. According to the detonation polar, this value is greater than the steady ODW angle. Thereafter, the wave angle decreases and asymptotes to the ODW angle of 31.5 deg.

As shown in Fig. 7 with the MoC results for $\theta < \theta_{CJ}$, CJ ODWs are initiated. The evolution of the wave angle for different wedge angles (from 4 to 15 deg) is shown in Fig. 9. The solid lines and the symbols refer to MoC and Amrita results, respectively. The horizontal dashed line represents the CJ ODW angle calculated from the Rankine–Hugoniot relations. For $\theta \geq 9$ deg, the agreement is reasonably good. For $\theta \leq 7$ deg, the evolution of the wave angle given by the MoC program differs from the numerical simulations because a shock wave was formed between the wedge and the attached oblique shock by the exothermic reactions. This shock was well simulated by the Amrita simulations. For the MoC simulations, characteristics crossed where the shock was formed. As explained already in this paper, the MoC program did not faithfully simulate such a shock formation, which explains the discrepancy between the MoC and Amrita results for the cases where a shock wave was formed in the domain of interest (which occurred for $\theta \leq 7$ deg). Despite this limitation with the MoC program, the wave angle reached the CJ value of 30.3 deg for wedge angles lower than θ_{CJ}. Because a CJ ODW was initiated even for very low wedge angles, it illustrates the fact that, for shock-induced combustion, a configuration where the reaction front remains uncoupled with the oblique shock in the far field is not a valid solution to the governing equations. For very low wedge angles, the induction distance may be very long, but once the reaction front is initiated, it unconditionally couples with the oblique shock to form a CJ ODW.

The wave structure obtained from Amrita simulations for deflection angles of $\theta = 11$ deg and 6 deg is presented in Fig. 10. A deflection angle of $\theta = 11$ deg is near the required value to form a CJ ODW ($\theta_{CJ} = 11.4$ deg). The ODW formation process is characterized by an inert oblique shock at the tip of the wedge followed by an induction zone. Chemical reactions form compression waves that strengthen the oblique shock and create a CJ ODW. The pressure contours are parallel to the shock front of the ODW. This process is observed for deflection angles in the range $\theta_{CJ} < \theta < \theta_{detach}$, and it is in accordance with the simulations and proposed wave structure of Li et al. [22]. Similar flow features can also be observed for a deflection angle of $\theta = 6$ deg (see Fig. 10b), with the exception that the pressure contours are no longer parallel behind the reaction zone of the ODW. At this location, the flow expands in order for the flow angle to become parallel to the wall. The expansion waves originate near the formation location of the ODW. This wave structure is in accordance with that proposed by Ashford and Emanuel [16].

B. Axisymmetric Configuration

The flowfield behind an inert conical shock attached to a cone can be described by the so-called Taylor–Maccoll flow [28]. The jump conditions across a conical shock are calculated in the same manner as an oblique shock. Behind the shock, the trajectory of the particles is curved, and the flow properties vary as they approach the cone surface. For a given shock angle, the corresponding cone angle is steeper than the corresponding wedge angle. For the construction of the detonation polar in the axisymmetric configuration, the structure of the ODW (or the jump conditions across the ODW) was assumed to be identical to that of the rectangular two-dimensional configuration. Between the end of the ODW reaction zone and the cone surface, the flow conditions were determined by solving the self-similar Taylor–Maccoll flow. This structure is valid far from the axis of symmetry where the radius of curvature is much larger than the thickness of the ODW reaction zone. Near the axis of symmetry, the curvature effect around the cone axis can, in principle, alter the ODW structure. This aspect will be addressed next.

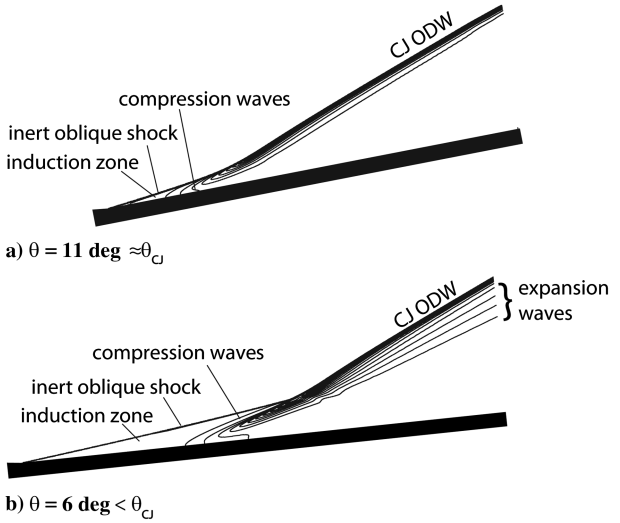

Fig. 10 Pressure contours from Amrita simulations showing the wave structure in the rectangular configuration. a) Deflection angle approximately equal to that required for a CJ oblique detonation. b) Deflection angle less than that required for a CJ oblique detonation.

Using the freestream conditions given by Eq. (2), the shock and detonation polars in the axisymmetric configuration are shown in Fig. 11, along with results from the MoC program. In the range $\theta_{CJ} < \theta < \theta_{detach}$, the agreement is again excellent. For $\theta < \theta_{CJ}$, CJ ODWs are initiated. The evolution of the wave angle for different cone angles (between 7 and 25 deg) obtained from the MoC program and Amrita is presented in Fig. 12. The ODW produced from the cone angle $\theta = 25$ deg is overdriven, whereas cone angles lower than $\theta_{CJ} = 21$ deg initiate CJ ODWs. In the axisymmetric configuration, the angle of the ODWs reaches a plateau where the reaction front couples with the oblique shock and continues to increase downstream of it towards the CJ value. Considering the cone angle of $\theta = 15$ deg, the plateau is at $140 < X < 180$, and in this range, the ODW angle is 26.7 deg. For $X > 180$, the ODW angle increases and presumably reaches the CJ value of 30.3 deg at very large X. The fact that an ODW can be initiated at an angle 3.6 deg lower than the CJ value is a result of the detonation front curvature. At $X = 160$, the curvature radius is smaller ($r_c = 61.4$) than at $X = 900$ ($r_c = 472$). Detonations with front curvature exhibit a velocity deficit with respect to their planar CJ velocity, a result that has been extensively investigated since the early study of Wood and Kirkwood [29]. In the case of an ODW, a velocity deficit translates into a reduction of the ODW angle to reduce the normal velocity component with respect to the ODW to below the CJ value. Therefore, the ODW angle is expected to be the lowest at the location of the smallest radius of curvature. In the far field, the curvature effect decreases and the ODW angle asymptotes to the angle of a planar CJ ODW.

It is of interest to compare the case of $\theta_{wedge} = 7$ deg from Fig. 9 with the case of $\theta_{cone} = 10$ deg from Fig. 12. For these two cases, the inert oblique shock angles are 13.4 deg and 13.3 deg for the rectangular and axisymmetric configurations, respectively. The strength of the oblique shock is thus approximately the same in the two configurations. It can be observed that the wave angle starts to increase at a similar location for the two cases (at approximately $X = 200$), but the wave angle increases more sharply in the rectangular configuration and overshoots the CJ wave angle before eventually relaxing to it. The ODW formation process for these two cases is presented in Fig. 13 with pressure contours from Amrita simulations. In the rectangular configuration, compression waves are formed near the end of the induction zone and sharply kink the inert oblique shock to a CJ ODW. Although the flow conditions on the wedge surface are the same as behind the oblique shock (near the beginning of the induction zone), this is not the case in the axisymmetric configuration. Because of the Taylor–Maccoll flow, the temperature on the cone surface is higher than behind the shock.

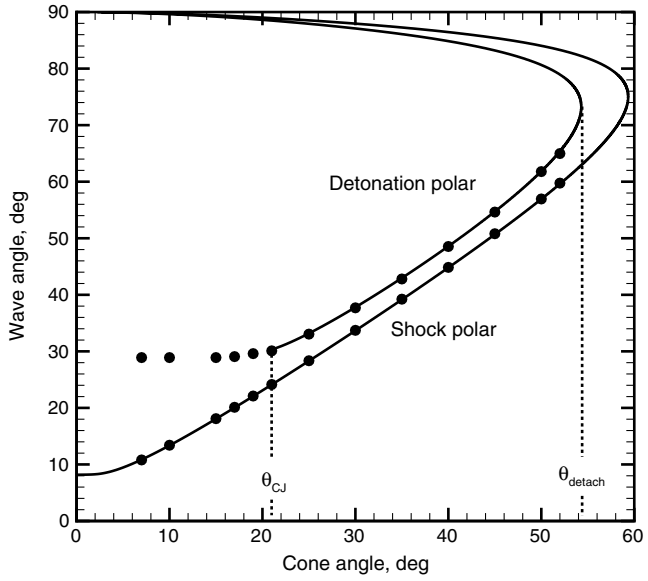

Fig. 11 Shock and detonation polars in the axisymmetric configuration. Symbols are MoC results.

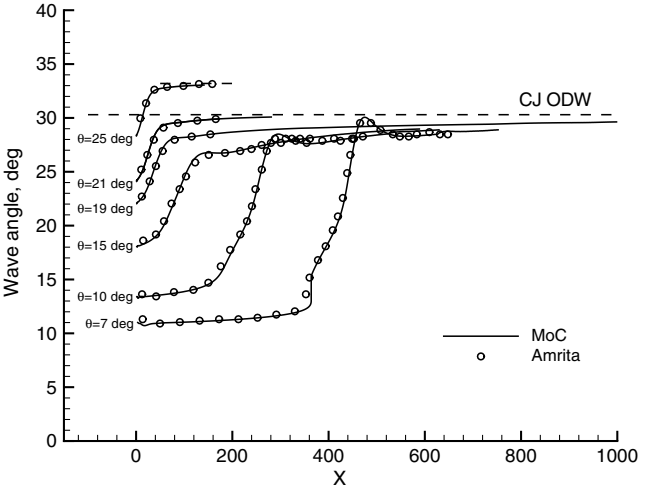

Fig. 12 Evolution of the wave angle, $7° < \theta < 25°$ in the axisymmetric configuration.

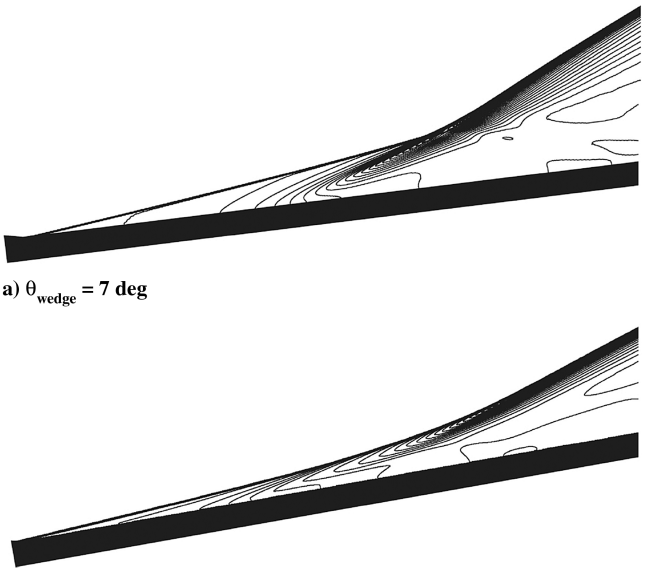

a) θ_{wedge} = 7 deg

b) θ_{cone} = 10 deg

Fig. 13 Pressure contours from Amrita simulations showing the ODW formation process a) in the rectangular configuration with a deflection angle of 7 deg and b) in the axisymmetric configuration with a deflection angle of 10 deg. In the two cases, the initial shock angle is the same.

Therefore, as observed in Fig. 13, the induction length along the wall is shorter in the axisymmetric configuration, and compression waves are formed closer to the tip, as compared with the rectangular configuration. As the reaction front propagates from the cone surface towards the shock, it passes through a series of streamlines of negative temperature gradient. This decreases the intensity of the reaction front, resulting in a more gradual increase of the wave angle.

IV. Conclusions

The present work is aimed at investigating the structure of oblique detonation waves (ODWs) using semi-infinite wedges and cones. The results were verified by comparing the oblique shock and ODW angles obtained from both theoretical and numerical simulations with shock and detonation polars. The wave structure for wedge angles equal to and less than θ_{CJ} was clarified. It is composed of an induction zone, the onset of a Chapman–Jouguet (CJ) ODW, and expansion waves that follow the end of the ODW reaction zone. Previous studies suggesting that steady oblique detonations may not exist with deflection angles less than that required for a CJ detonation

neglected the fact that a detonation, once initiated, is able to propagate independently of downstream conditions. Thus, downstream of an initiation process, an oblique CJ detonation can exist on wedges and cones with deflection angles $\theta < \theta_{CJ}$, with an expansion fan downstream of the reaction zone matching the flow angle with that of the wall. Simulations of reactive flows over cones revealed that the intensity of the reaction front and the compression waves generated in the ODW initiation process were decreased, in comparison with the planar wedge cases. Also, the effect of curvature within the reaction zone allowed ODWs to be initiated at angles less than the CJ value.

This investigation is of primary importance to hypersonic propulsion because it shows that, under ideal conditions (neglecting thermal and viscous transport effects and modeling the chemistry with a single irreversible reaction), ODWs can be stabilized on very low wedge and cone angles, hence minimizing the associated pressure drag of the body. Under realistic conditions and detailed chemistry, it is possible that competing effects (such as heat losses through the wall) would prevent exothermic reactions to be triggered behind very low shock angles. Nevertheless, if the thermal runaway occurs at any location on the wedge or cone surface, the reaction front would eventually couple to the oblique shock, unless it is quenched by a corner-generated expansion. The physical dimension of the induction zone could also be obtained with this type of analysis. To determine whether an ODW or a ram accelerator should operate in the uncoupled shock-induced combustion regime or in the ODW regime is left to a separate investigation.

Acknowledgments

This work was sponsored by Defence Research and Development Canada—Valcartier. Matei Radulescu and James Quirk are thanked for their assistance with the Amrita simulations.

References

[1] Dunlap, R., Brehm, R. L., and Nicholls, J. A., "Preliminary Study of the Application of Steady-State Detonative Combustion to a Reaction Engine," *Jet Propulsion*, Vol. 28, No. 7, 1958, pp. 451–456.

[2] Dudebout, R., Sislian, J. P., and Oppitz, R., "Numerical Simulation of Hypersonic Shock-Induced Combustion Ramjets," *Journal of Propulsion and Power*, Vol. 14, No. 6, 1998, pp. 869–879. doi:10.2514/2.5368

[3] Parent, B. and Sislian, J. P., "Effect of Geometrical Parameters on the Mixing Performance of Cantilevered Ramp Injectors," *AIAA Journal*, Vol. 41, No. 3, 2003, pp. 448–456. doi:10.2514/2.1966

[4] Schwartzentruber, T., Sislian, J. P., and Parent, B., "Suppression of Premature Ignition in the Premixed Inlet Flow of a Shcramjet," *Journal of Propulsion and Power*, Vol. 22, No. 10, 2006, pp. 2145–2155.

[5] Sislian, J. P., Martens, R. P., Schwartzentruber, T. E., and Parent, B., "Numerical Simulation of a Real Shcramjet Flowfield," *Journal of Propulsion and Power*, Vol. 22, No. 5, 2006, pp. 1039–1048. doi:10.2514/1.14895

[6] Chan, J., Sislian, J. P., and Alexander, D. C., "Numerically Simulated Comparative Performance of a Scramjet and Shcramjet at Mach 11," *Journal of Propulsion and Power*, Vol. 26, No. 5, 2010, pp. 1125–1134. doi:10.2514/1.48144

[7] Hertzberg, A., Bruckner, A. P., and Bogdanoff, D. W., "Ram Accelerator: a New Chemical Method for Accelerating Projectiles to Ultrahigh Velocities," *AIAA Journal*, Vol. 26, No. 2, 1988, pp. 195–203. doi:10.2514/3.9872

[8] Higgins, A. J., "Ram Accelerators: Outstanding Issues and New Directions," *Journal of Propulsion and Power*, Vol. 22, No. 6, 2006, pp. 1170–1187. doi:10.2514/1.18209

[9] Shepherd, J. E., "Detonation Waves and Propulsion," *Combustion in High-Speed Flows*, edited by J. Buckmaster, T. L. Jackson and A. Kumar, Kluwer Academic, Norwell, MA, 1994, pp. 373–420.

[10] Powers, J. M., "Oblique Detonations: Theory and Propulsion Applications," *Combustion in High-Speed Flows*, edited by J. Buckmaster, T. L. Jackson and A. Kumar, Kluwer Academic, Norwell, MA, 1994, pp. 345–371.

[11] Siestrunck, R., Fabri, J. and Le Grives, E., "Some Properties of Stationary Detonation Waves," *Symposium (International) on Combustion : [papers]*, Vol. 4, No. 1, 1953, pp. 498–501.

[12] Larisch, E., "Interactions of Detonation Waves," *Journal of Fluid Mechanics*, Vol. 6, No. 3, 1959, pp. 392–400. doi:10.1017/S0022112059000714

[13] Gross, R. A., "Oblique Detonation Waves," *AIAA Journal*, Vol. 1, No. 5, 1963, pp. 1225–1227. doi:10.2514/3.1777

[14] Pratt, D. T., Humphrey, J. W., and Glenn D. E., "Morphology of Standing Oblique Detonation Waves," *Journal of Propulsion and Power*, Vol. 7, No. 5, 1991, pp. 837–845. doi:10.2514/3.23399

[15] Buckmaster, J. and Lee, C. J., "Flow Refraction by an Uncoupled Shock and Reaction Front," *AIAA Journal*, Vol. 28, No. 7, 1990, pp. 1310–1312. doi:10.2514/3.25211

[16] Ashford, S. A. and Emanuel, G., "Wave Angle for Oblique Detonation Waves," *Shock Waves*, Vol. 3, No. 4, 1994, pp. 327–329. doi:10.1007/BF01415831

[17] Emanuel, G. and Tuckness, D. G., "Steady, Oblique, Detonation Waves," *Shock Waves*, Vol. 13, No. 6, 2004, pp. 445–451.

[18] Powers, J. M. and Gonthier, K. A., "Reaction Zone Structure for Strong, Weak Overdriven, and Weak Underdriven Oblique Detonations," *Physics of Fluids A*, Vol. 4, No. 9, 1992, pp. 2082–2089. doi:10.1063/1.858378

[19] Fickett, W., and Davis, W. C., *Detonation*, Univ. of California Press, Berkeley, CA, 1979, pp. 168–173.

[20] Lee, J. H. S., *The Detonation Phenomenon*, Cambridge Univ. Press, New York/London/ Cambridge, England, U.K., 2008, pp. 83–89.

[21] Desbordes, D., Hamada, L., and Guerraud, C., "Supersonic H_2-air Combustions Behind Oblique Shock Waves," *Shock Waves*, Vol. 4, No. 6, 1995, pp. 339–345. doi:10.1007/BF01413876

[22] Li, C., Kailasanath, K., and Oran, E. S., "Detonation Structures Behind Oblique Shocks," *Physics of Fluids*, Vol. 6, No. 4, 1994, pp. 1600–1611. doi:10.1063/1.868273

[23] Ghorbanian, K., and Sterling, J. D., "Influence of Formation Processes on Oblique Detonation Wave Stabilization," *Journal of Propulsion and Power*, Vol. 12, No. 3, 1996, pp. 509–517. doi:10.2514/3.24064

[24] Verreault, J., and Higgins, A. J., "Initiation of Detonation by Conical Projectiles," *Proceedings of the Combustion Institute*, Vol. 33, No. 2, 2011, pp. 2311–2318. doi:10.1016/j.proci.2010.07.086

[25] Quirk, J. J., "Amrita—A Computational Facility for CFD Modelling," *29th Computational Fluid Dynamics* [online edition], VKI Lecture Series, edited by H. Deconinck, www.amrita-cfd.org/cgi-bin/doc/vki [retrieved 3 June 2012].

[26] Lee, H. I., and Stewart, D. S., "Calculation of Linear Detonation Instability: One-Dimensional Instability of Plane Detonation," *Journal of Fluid Mechanics*, Vol. 216, 1990, pp. 103–132. doi:10.1017/S0022112090000362

[27] Zucrow, M. J. and Hoffman, J. D., *Gas Dynamics, Vol. II: Multidimensional Flow*, Wiley, New York, 1977, pp. 185–266.

[28] Anderson, J. D., *Modern Compressible Flow: With Historical Perspective*, 2nd ed., McGraw–Hill, New York, 2002, pp. 294–306.

[29] Wood, W. W., and Kirkwood, J. G., "Diameter Effect in Condensed Explosives: The Relation Between Velocity and Radius of Curvature of the Detonation Wave," *Journal of Chemical Physics*, Vol. 22, No. 11, 1954, pp. 1920–1924. doi:10.1063/1.1739940

J. Drummond
Associate Editor